

CHAPTER 4 BEAT PHENOMENON

*It is far easier to write differential equations than to perceive
the nature of their solutions -- if the latter exist at all.
- Anonymous*

This chapter examines a phenomenon which occurs very commonly in combined structure-liquid damper systems. Transfer of energy takes place in the coupled system which could induce vibrations in the primary structure instead of suppressing them. This chapter focusses on understanding the phenomenon from a mathematical point of view. Numerical and experimental results are presented in this chapter to elucidate the *beat phenomenon* in combined structure-liquid damper systems.

4.1 Introduction

The *beat phenomenon* has been discussed in many classical texts on vibration (e.g., Den Hartog, 1956). Figure 4.1 shows coupling present in different mechanical and electrical systems. It is well known that beats occur when two frequencies are close together. This usually occurs when the coupling is very soft in comparison to the main “springs”. In an electrical analogue, this means larger capacitance of the coupling than the main capacitances. Transfer of energy takes place in the coupled system which could induce vibration in the primary system instead of suppressing them.

Experimental studies involving a TLCD combined with a simple structure have provided insightful understanding into the behavior of liquid damper systems. The motivation of this paper is portrayed in Figs. 4.2 (a) and (b), which show the free vibration decay

of a combined structure-TLD and -TLCD in the laboratory. The controlled response exhibits the classical *beat phenomenon* characterized by a modulated instead of an exponential decay in the signature.

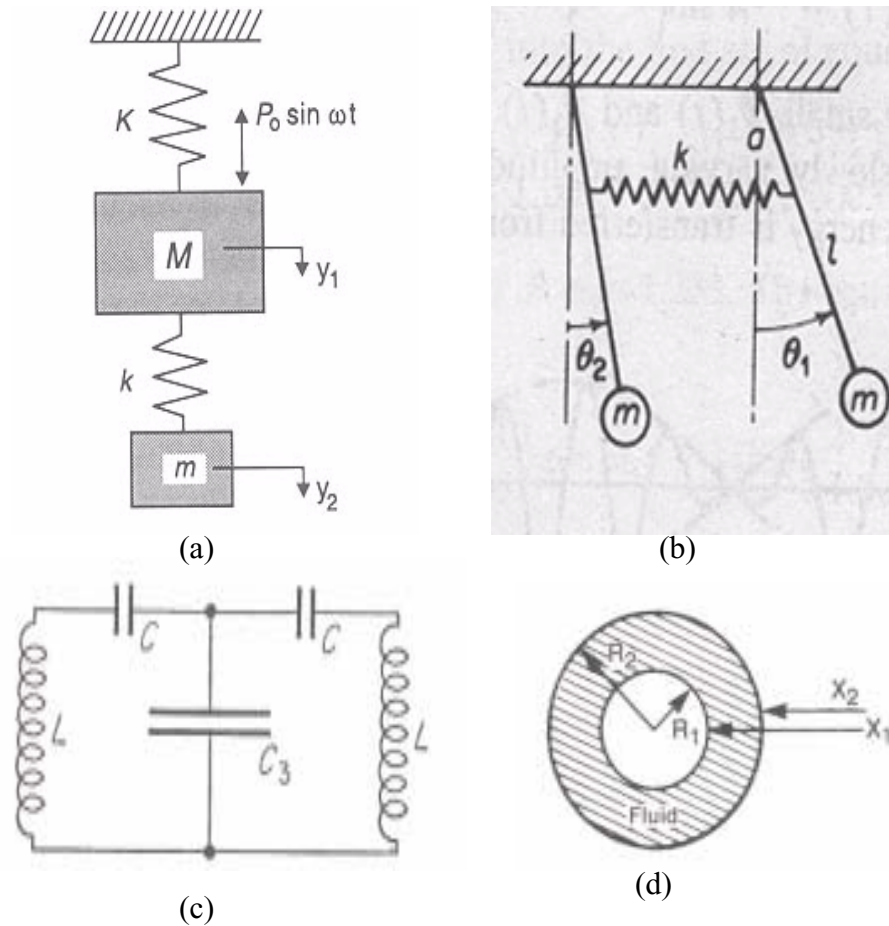
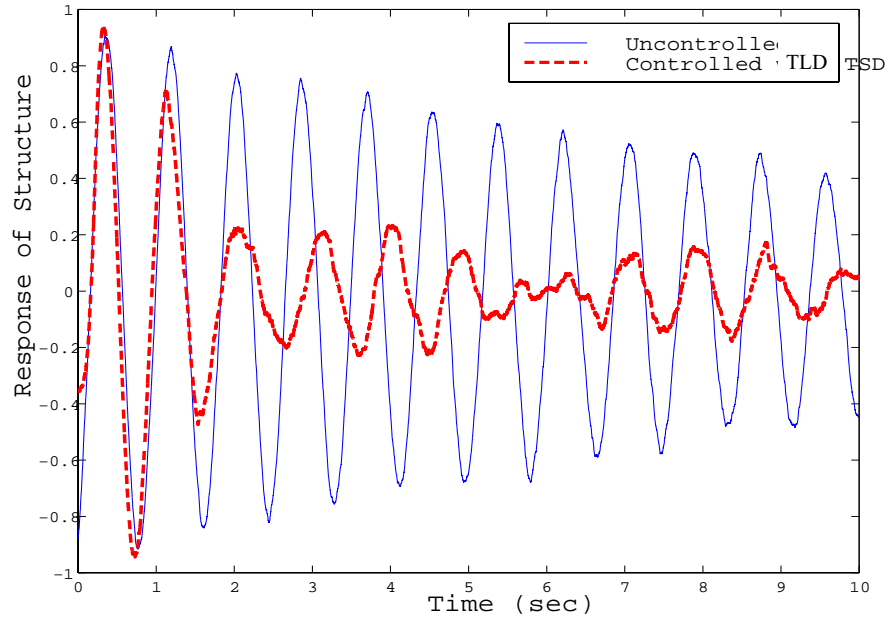


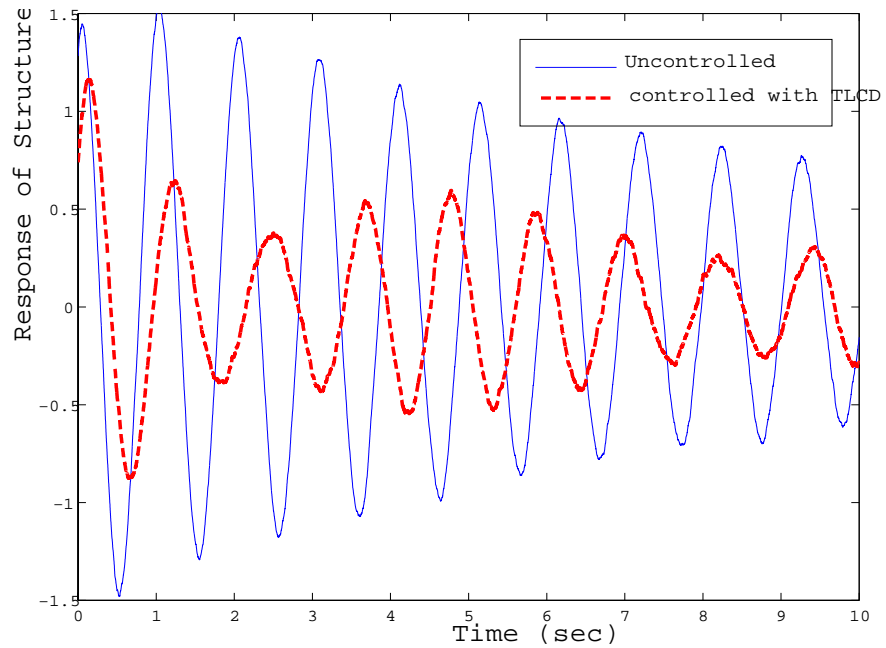
Figure 4.1 Different coupled system (a) Vibration absorber (b) Coupled penduli system (c) Electrical system (d) Fluid coupling within two cylinders

However, beyond a certain level of damping in the TLCD, this beat phenomenon ceases and the structural response resembles a SDOF decay. Of course, as a limiting case one might expect this to happen because when the damping is very high in the secondary system, the combined system essentially behaves as a SDOF system. However, the critical damping at which this disappearance of beat phenomenon is initiated is not understood.

This chapter delves into better understanding the *beat phenomenon* for the combined structure-TLCD system.



(a)



(b)

Figure 4.2 Uncontrolled and Controlled response of a structure combined with (a) TLD (b) TLCD

4.2 Behavior of SDOF system with TLCD

In this section, three different cases are considered as shown in Fig. 4.3. These are undamped combined system; damped primary system with undamped secondary system; and damped primary and secondary system. We will look at each case in detail. In order to keep the discussion general, the subscripts 1 and 2 are introduced instead of s for structure and f for the damper, as in Chapter 3.

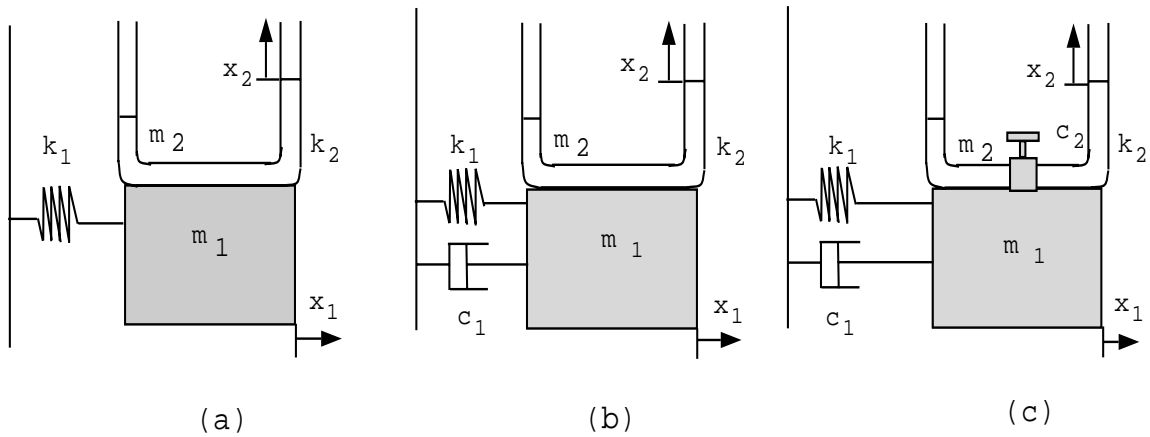


Figure 4.3 Different combined systems

4.2.1 Case 1: Undamped Combined System

The coupled equations of motion without damping in the primary and secondary system (Fig 4.3 (a)) can be obtained from Eq. 3.6 by setting damping in each system equal to zero,

$$\begin{bmatrix} 1 + \mu & \alpha\mu \\ \alpha & 1 \end{bmatrix} \begin{bmatrix} \ddot{x}_1 \\ \ddot{x}_2 \end{bmatrix} + \begin{bmatrix} \omega_1^2 & 0 \\ 0 & \omega_2^2 \end{bmatrix} \begin{bmatrix} x_1 \\ x_2 \end{bmatrix} = \begin{bmatrix} 0 \\ 0 \end{bmatrix} \quad (4.1)$$

The modal frequencies of this system are given by:

$$\bar{\omega}_{1,2} = \sqrt{\frac{\omega_1^2 + \omega_2^2(1 + \mu) \pm \Pi}{2(1 + \mu - \alpha^2\mu)}} \quad (4.2)$$

where $\Pi^2 = (\omega_1^2 - \omega_2^2(1 + \mu))^2 + 4\omega_1^2\omega_2^2\alpha^2\mu$

It is obvious from Eq. 4.2 that, for an uncoupled system (i.e., for $\alpha=0$), the eigenvalues reduce to:

$$\bar{\omega}_1 = \frac{\omega_1}{\sqrt{1 + \mu}}; \bar{\omega}_2 = \omega_2 \quad (4.3)$$

The coupling parameter α in the mass matrix is responsible for the *beat phenomenon*. Figure 4.4 shows the phase plane portraits for the primary system for different values of α . Unless mentioned otherwise, all units of displacements, frequencies and velocities are *m*, *rad/sec* and *m/sec*, respectively. The first portrait shows that with no coupling there is only one frequency at which the structure responds, and as the coupling parameter increases there is *interference* between the two states of the primary system, namely, x_1 and \dot{x}_1 .

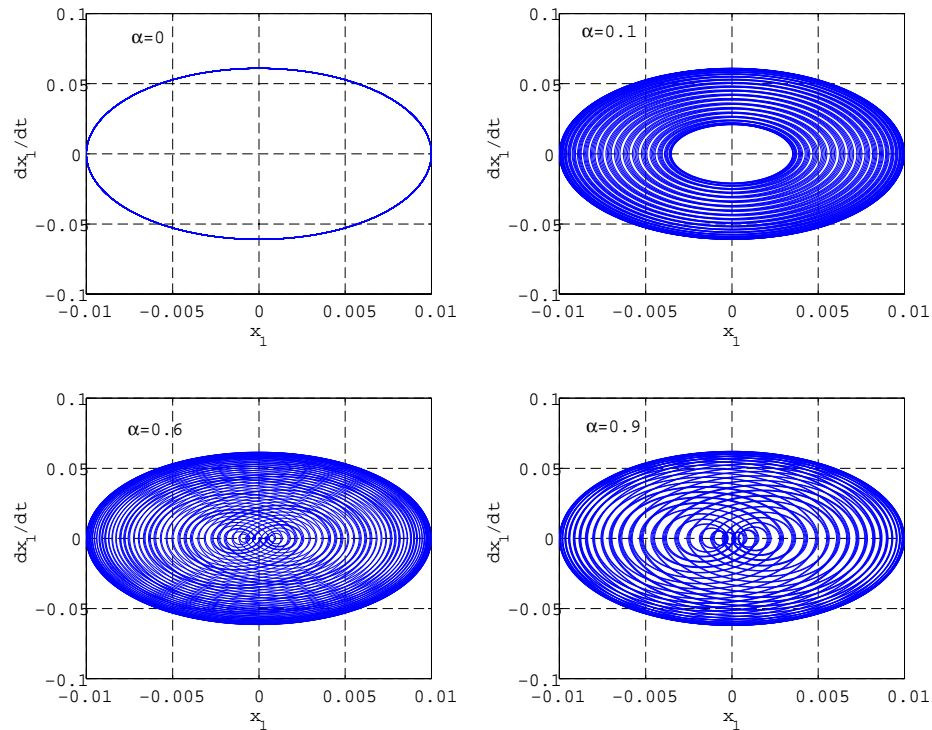


Figure 4.4 Phase plane portraits of the undamped coupled system

For all simulations in this chapter, the following parameters have been kept constant, $\omega_1=1$ Hz, $\mu=0.01$ and $\omega_2=0.99$ Hz. Figure 4.5 shows the time histories of the displacement of the undamped primary system for $\alpha=0$ and $\alpha=0.6$. When coupling is present between the two systems, the displacement signature is amplitude modulated.

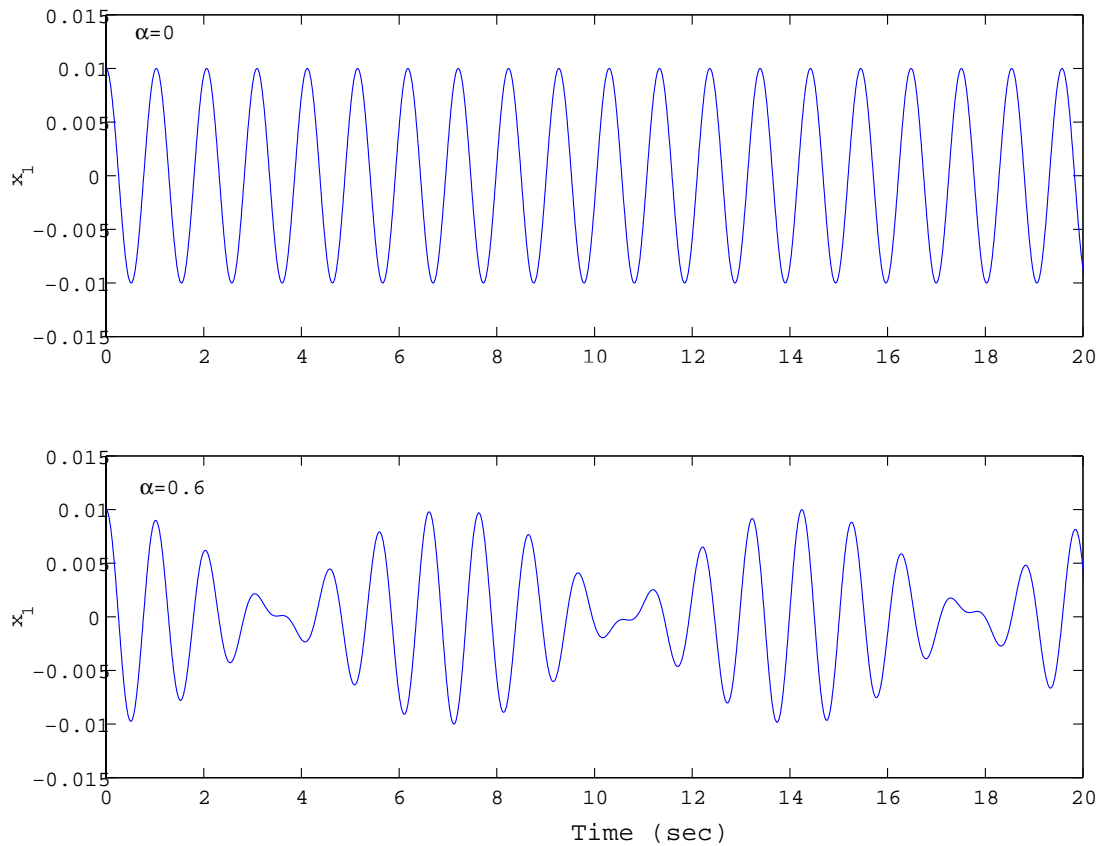


Figure 4.5 Time histories of primary system displacement for $\alpha=0$ and $\alpha=0.6$

To understand this phenomenon better, one can consider the solution of the system of equations given in Eq. 4.1. After some mathematical manipulation the displacement of the primary system for the initial conditions, $x_1(0) = x_0$; $x_2(0) = 0$; $\dot{x}_1(0) = 0$ and $\dot{x}_2(0) = 0$, is given by:

$$x_1(t) = x_0 \cos\left(\frac{\omega_B t}{2}\right) \cos\left(\frac{\omega_A t}{2}\right) \quad (4.4)$$

where $\omega_A = \bar{\omega}_1 + \bar{\omega}_2$ and $\omega_B = \bar{\omega}_2 - \bar{\omega}_1$, which means that the resulting function is an amplitude-modulated harmonic function with a frequency equal to ω_B and the amplitude varying with a frequency of ω_A . This undamped combined system case has been examined in texts on vibration (e.g., Den Hartog, 1956).

4.2.2 Case 2: Linearly Damped Structure with Undamped Secondary System

In this section, a linearly damped primary system with undamped secondary system as shown in Fig. 4.3(b) is considered. Accordingly, the equations of motion are given by:

$$\begin{bmatrix} 1 + \mu & \alpha\mu \\ \alpha & 1 \end{bmatrix} \begin{bmatrix} \ddot{x}_1 \\ \ddot{x}_2 \end{bmatrix} + \begin{bmatrix} 2\omega_1\zeta_1 & 0 \\ 0 & 0 \end{bmatrix} \begin{bmatrix} \dot{x}_1 \\ \dot{x}_2 \end{bmatrix} + \begin{bmatrix} \omega_1^2 & 0 \\ 0 & \omega_2^2 \end{bmatrix} \begin{bmatrix} x_1 \\ x_2 \end{bmatrix} = \begin{bmatrix} 0 \\ 0 \end{bmatrix} \quad (4.5)$$

This system has two complex conjugate pairs of eigenvalues,

$$\lambda_{1,2} = -\bar{\omega}_1\tilde{\zeta}_1 \pm i\bar{\omega}_1\sqrt{1 - \tilde{\zeta}_1^2} \quad \text{and} \quad \lambda_{3,4} = -\bar{\omega}_2\tilde{\zeta}_2 \pm i\bar{\omega}_2\sqrt{1 - \tilde{\zeta}_2^2},$$

where $\bar{\omega}_{1,2}$ are the modal frequencies and $\tilde{\zeta}_{1,2}$ are the modal damping ratios. The average frequency and the beat frequency are plotted in Fig. 4.6 for different damping ratios of the primary system. At $\alpha = 0$, the beat frequency (i.e. the difference in modal frequencies) tends to be zero. As the coupling is increased, there is an increase in the beat frequency which causes the *beat phenomenon*. From this analysis, one can conclude that there is no *beat phenomenon* when the difference in the modal frequencies approaches zero. Figure 4.6 also shows the effect of introducing damping in the primary system. At high levels of damping ratio, there is a wider range of coupling term α which results in the beat frequency being equal to zero. This means that, over this range of the coupling term, there is

hardly any *beat phenomenon*. For $\alpha = 0.3$, *beat phenomenon* is present when the damping ratio in the primary system is 0.005, but it disappears when the damping ratio is 0.05. Figure 4.7 shows the effect of damping in the primary system on the response of the primary system. As the damping ratio increases, the response dies out in an exponential decay. However, the *beat phenomenon* still exists. This poses difficulty in the estimation of system damping from free vibration response time histories.

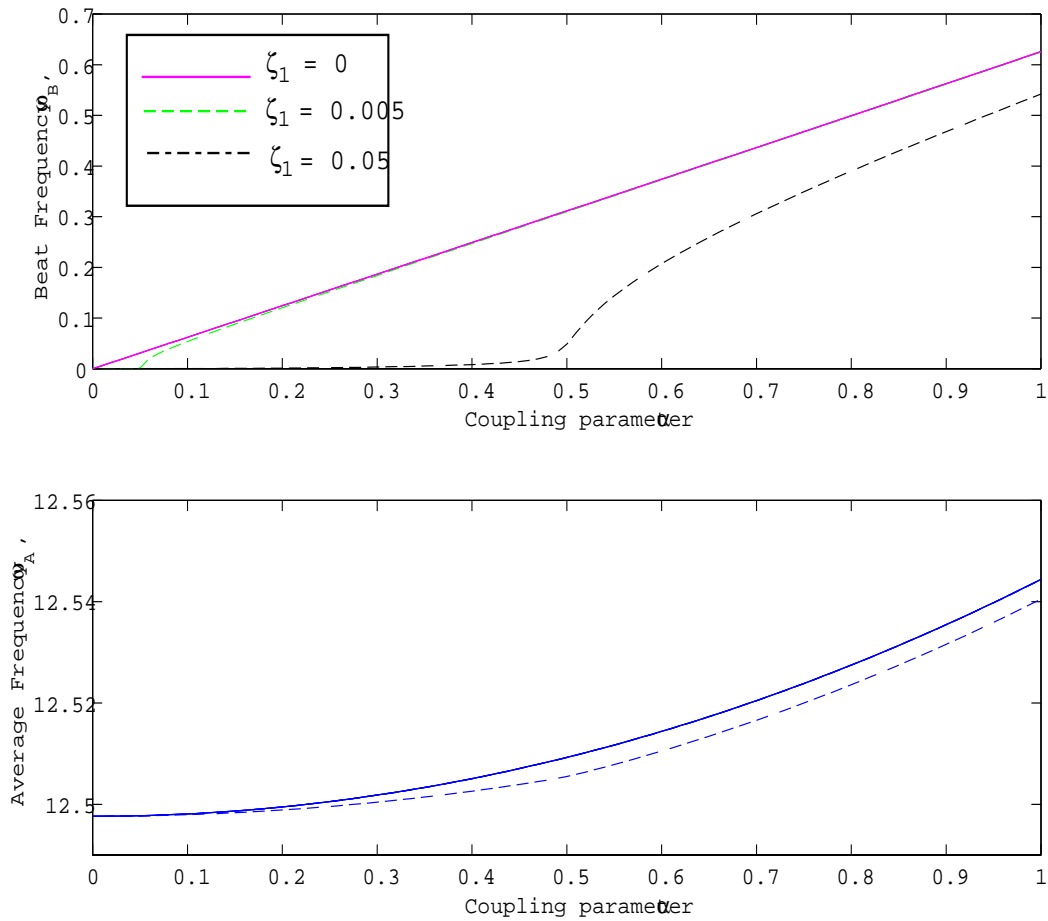


Figure 4.6 Variation of ω_A and ω_B as a function of α

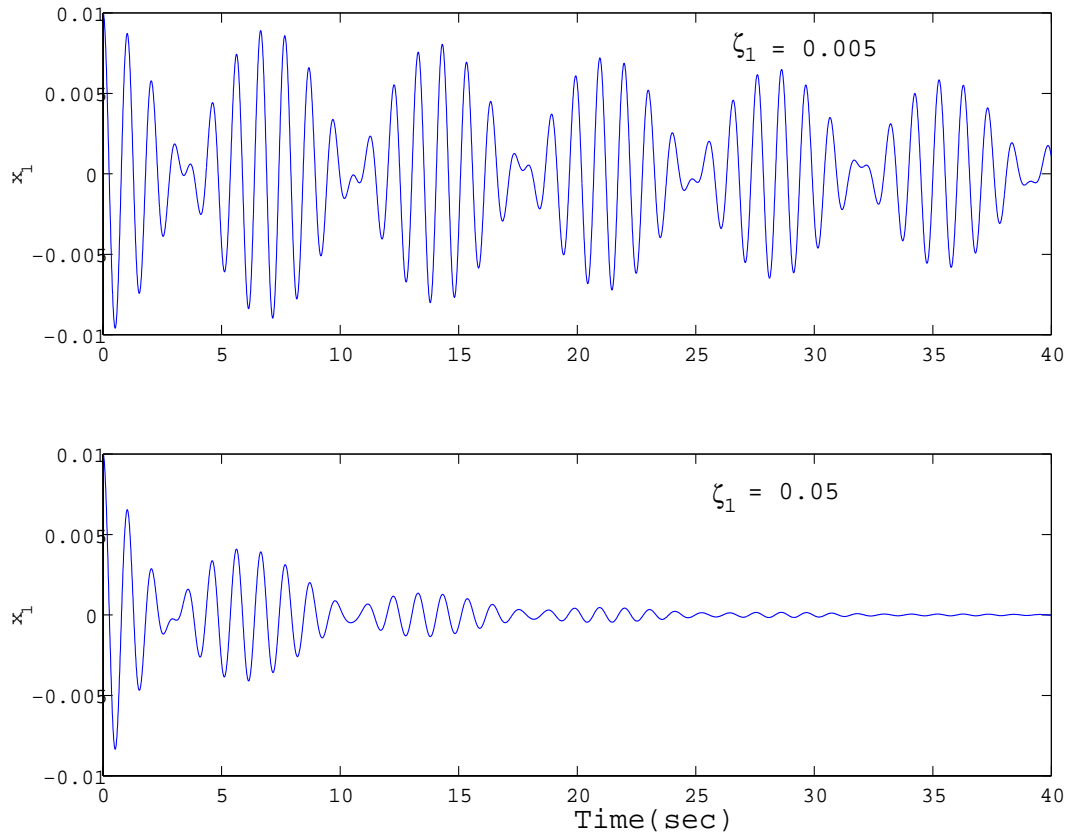


Figure 4.7 Time histories of response for $\zeta_1=0.005$ and $\zeta_1=0.05$

At this stage, the effect of a decrease in beat frequency on the response signal can be further examined. Figure 4.8 shows that as ω_B approaches zero, T_B (the time period of the beat frequency) becomes very large. The parameter influencing the decay function is Ψ (for a SDOF system, $\Psi = \zeta_1 \omega_1$). As a result, due to the damping in the primary system, the response dies out before the next peak of the beat cycle arises. Therefore, the response resembles that of a damped SDOF system.

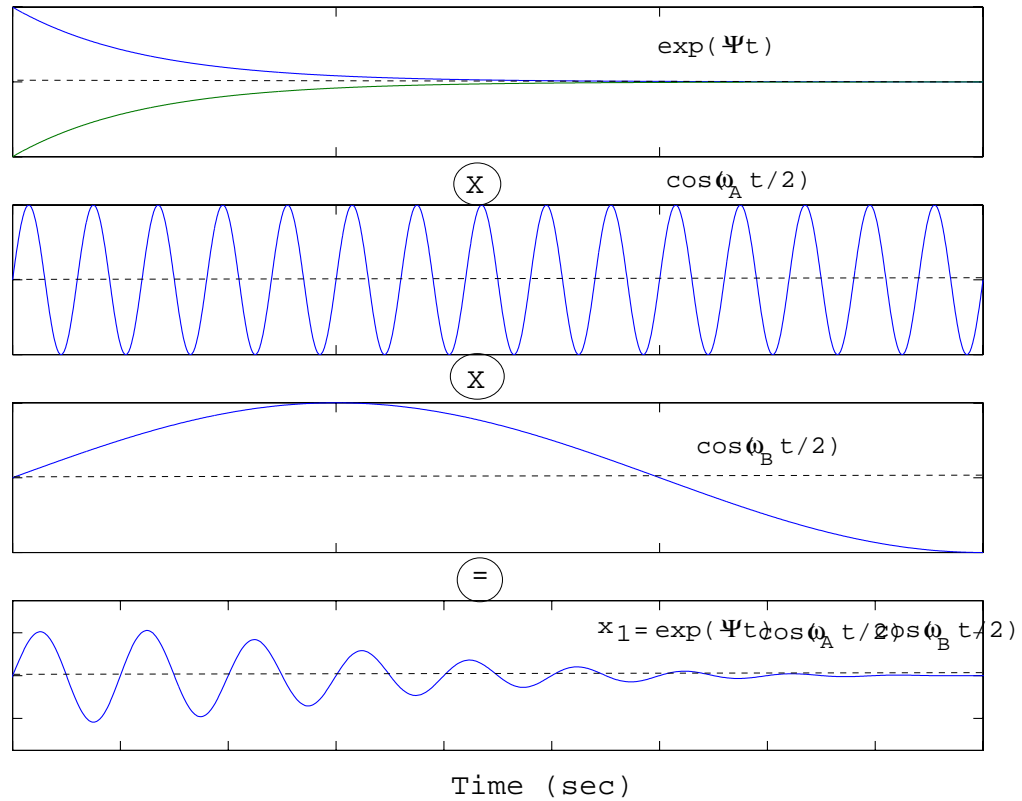


Figure 4.8 Anatomy of the damped response signature

4.2.3 Case 3: Damped Primary and Secondary System

In this section, the system represented by Fig 4.3 (c) is considered, where now an orifice in the middle of the U-tube imparts damping to the system. In this case, the following equations of motion apply:

$$\begin{bmatrix} 1 + \mu & \alpha\mu \\ \alpha & 1 \end{bmatrix} \begin{bmatrix} \ddot{x}_1 \\ \ddot{x}_2 \end{bmatrix} + \begin{bmatrix} 2\omega_1\zeta_1 & 0 \\ 0 & \omega_2^2\xi|\dot{x}_2|/4g \end{bmatrix} \begin{bmatrix} \dot{x}_1 \\ \dot{x}_2 \end{bmatrix} + \begin{bmatrix} \omega_1^2 & 0 \\ 0 & \omega_2^2 \end{bmatrix} \begin{bmatrix} x_1 \\ x_2 \end{bmatrix} = \begin{bmatrix} 0 \\ 0 \end{bmatrix} \quad (4.6)$$

where ξ is the headloss coefficient and $c_2 = \frac{1}{2}\rho A\xi$. Equation 4.6 is numerically integrated at different levels of the headloss coefficient and setting $\zeta_1 = 0.001$ and $\alpha=0.3$ (Fig 4.9).

The figure shows an interesting behavior of the liquid damper system. In the previous sec-

tion, the damping simply caused an exponential decay of the beat response. However, in this case, the *beat phenomenon* disappears after a certain level of the headloss coefficient. Since an analytical solution is not convenient for this equation due to the quadratic nonlinearity in the damping associated with the secondary system, a linearized version (see section 3.2.1) of this system is generally considered. Therefore, Eq. 4.6 is recast as:

$$\begin{bmatrix} 1 + \mu & \alpha\mu \\ \alpha & 1 \end{bmatrix} \begin{bmatrix} \dot{x}_1 \\ \dot{x}_2 \end{bmatrix} + \begin{bmatrix} 2\omega_1\zeta_1 & 0 \\ 0 & 2\omega_2\zeta_2 \end{bmatrix} \begin{bmatrix} \dot{x}_1 \\ \dot{x}_2 \end{bmatrix} + \begin{bmatrix} \omega_1^2 & 0 \\ 0 & \omega_2^2 \end{bmatrix} \begin{bmatrix} x_1 \\ x_2 \end{bmatrix} = \begin{bmatrix} 0 \\ 0 \end{bmatrix} \quad (4.7)$$

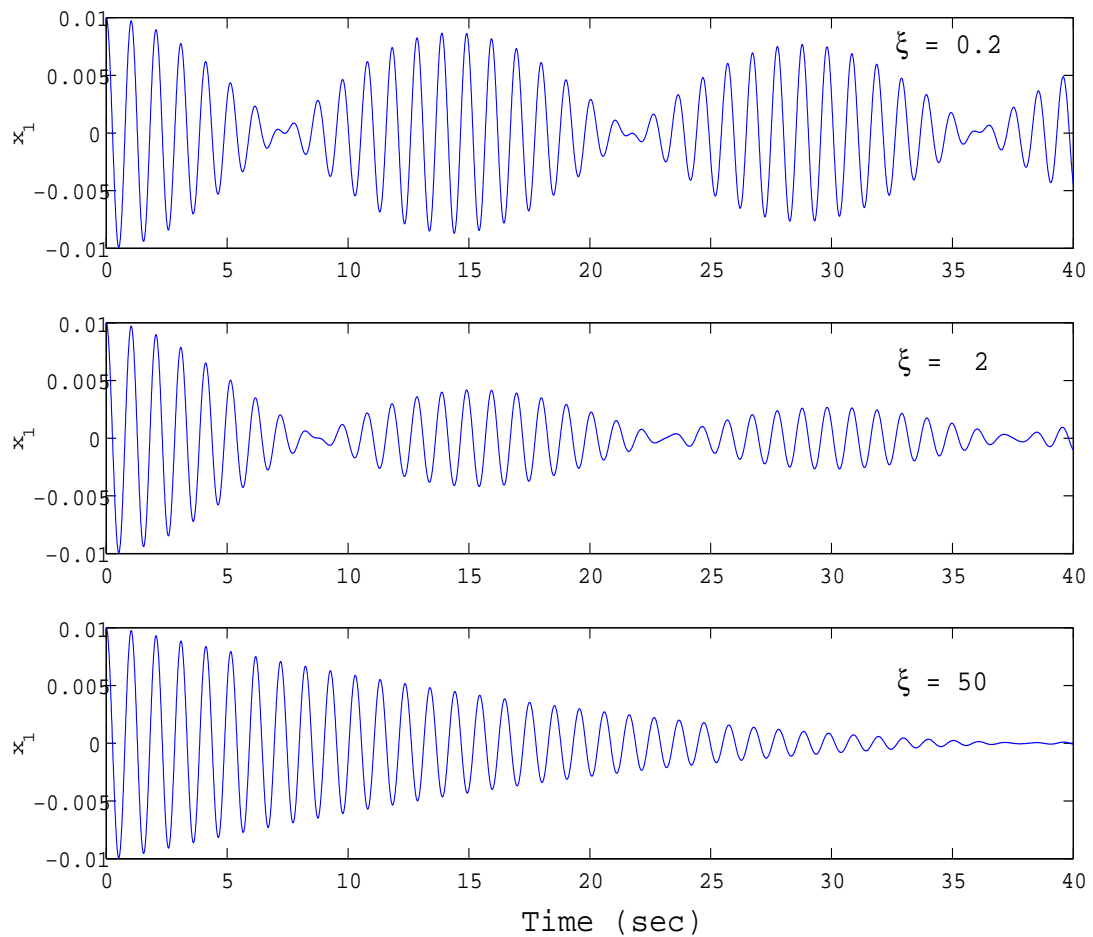


Figure 4.9 Time histories of response for $\xi=0.2, 2$ and 50

The modal frequencies and damping ratios of the system defined in Eq. 4.7 are plotted in Fig. 4.10 as a function of equivalent damping ratio, ζ_2 . Figure 4.10 explains the disappearance of the *beat phenomenon* due to coalescing of the modal frequencies after a certain value of the equivalent damping ratio. As seen in the previous chapter, this change in equivalent damping ratio is realized through changing of the headloss coefficient. The resulting beat frequency approaches zero and hence *beat phenomenon* ceases to exist. This is similar to a previous case where there was no *beat phenomenon* for coupling term $\alpha = 0$, in which case the beat frequency was zero.

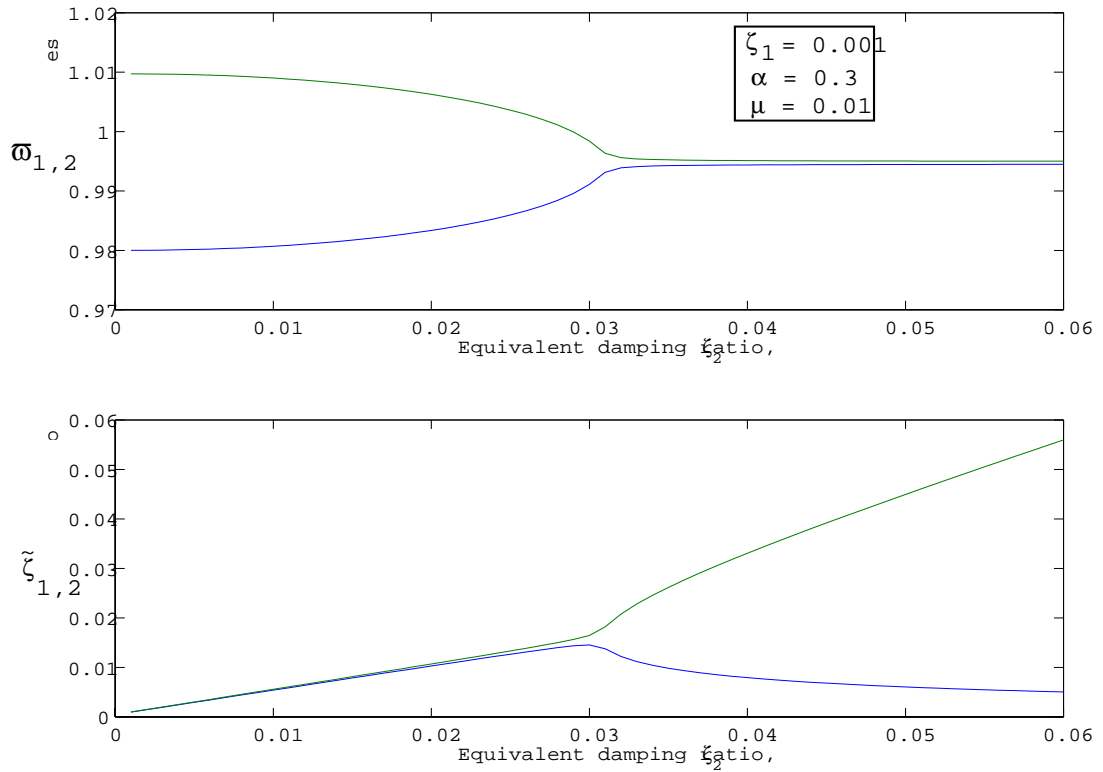


Figure 4.10 Modal frequencies and modal damping ratios of combined system as a function of the damping ratio of the TLCD

Figure 4.11 shows the three dimensional plots of state space portraits as a function of time. Figure 4.11(a) shows the evolution for an uncoupled system in which the amplitude of response is constant. Figures 4.11(b) and (c) show the cases discussed in sections 4.2.1 and 4.2.2. The final plot, Fig. 4.11(d), shows case 3 in which no *beat phenomenon* occurs in the coupled system.

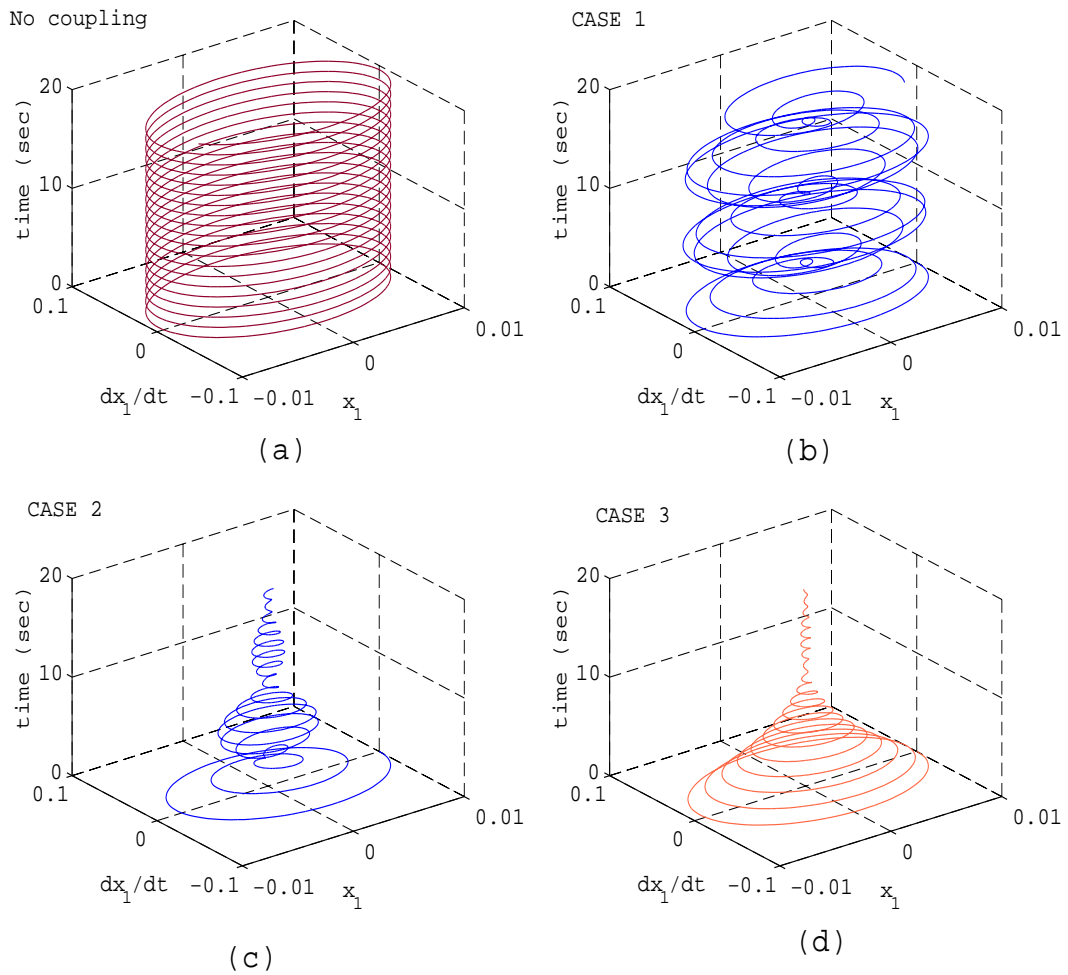


Figure 4.11 Phase-plane 3D plots (a) uncoupled system (b) case 1: undamped system (c) case 2: system with damping in primary system only (d) case 3: system with damping in both primary and secondary systems

4.3 Experimental Verification

In order to further validate the observations made in section 4.2, a simple experiment was conducted using the experimental setup shown in Fig. 4.12. A TLCD is mounted on a SDOF structure. The TLCD was designed with a variable orifice, to effectively change the headloss coefficient. At $\theta = 0$ degrees, the valve is fully opened and the headloss is increased with an increase in the angle of rotation, θ . In Fig. 4.13, one can note the presence of a *beat* pattern for low headloss coefficients. However, as the headloss coefficient is increased, the *beat phenomenon* disappears and an exponentially decaying signature is obtained. A similar observation was made in Fig. 4.9 for simulated time histories.

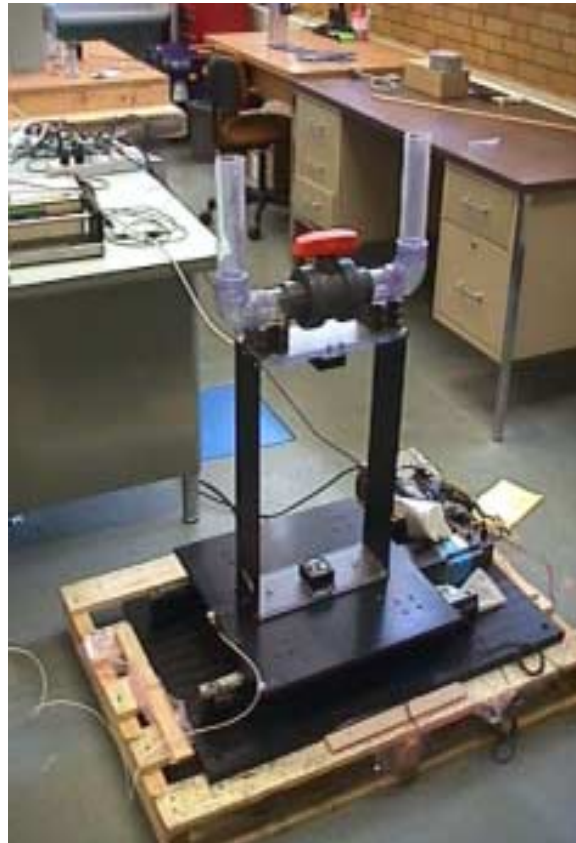


Figure 4.12 Experimental setup for combined structure-TLCD system on a shaking table

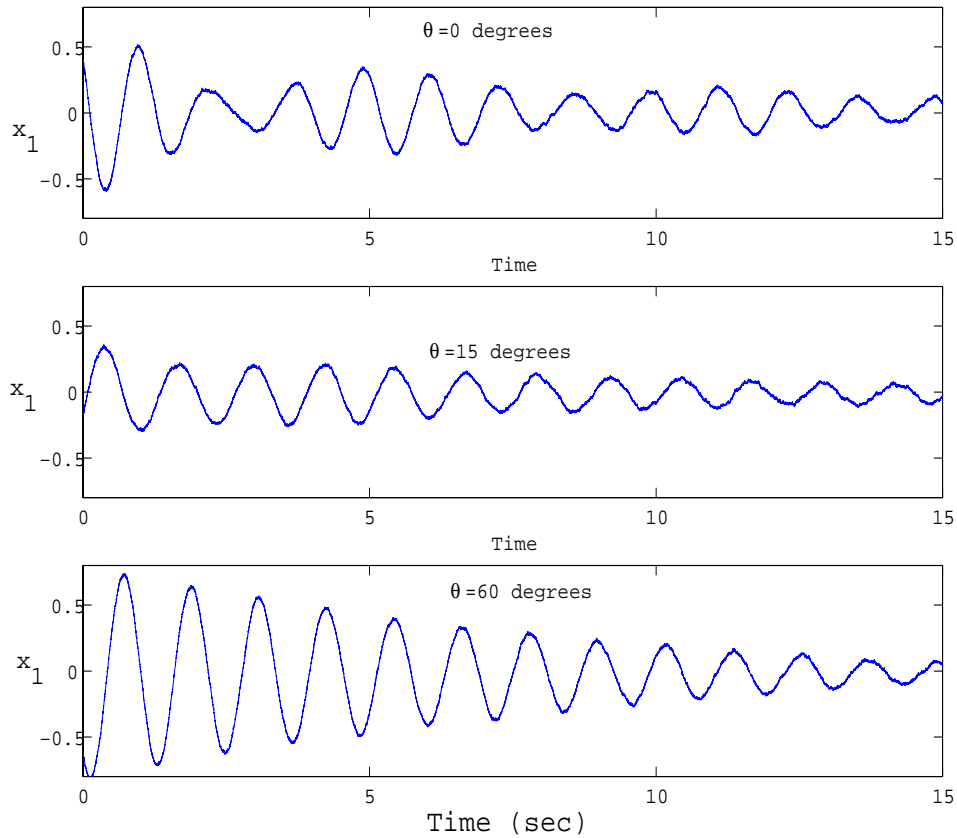
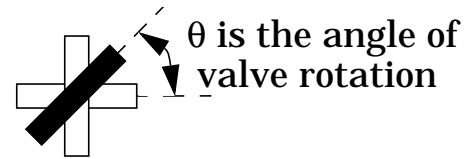


Figure 4.13 Experimental free vibration response with different orifice openings ($\theta = 0$ fully open)

4.4 Concluding Remarks

Similar to coupled mechanical systems, the combined structure-liquid damper system exhibits the *beat phenomenon* due to the coupling term that appears in the mass matrix of the combined system. The free vibration structural response resembles an amplitude modulated signal. The beat frequency of the modulated signature is given by the difference in the modal frequencies of the coupled system. However, beyond a certain level of damping in the secondary system (liquid damper), the *beat phenomenon* ceases to exist. This is

attributed to the coalescing of the modal frequencies of the combined system to a common frequency beyond a certain level of damping in the secondary system.